



ELSEVIER

Nuclear Instruments and Methods in Physics Research A 479 (2002) 548–554

**NUCLEAR  
INSTRUMENTS  
& METHODS  
IN PHYSICS  
RESEARCH**  
Section A

www.elsevier.com/locate/nima

# Evolution of silicon microstrip detector currents during proton irradiation at the CERN PS

R.S. Harper<sup>a,\*</sup>, C.M. Buttar<sup>a</sup>, P.P. Allport<sup>b</sup>, L. Andricek<sup>c</sup>, J.R. Carter<sup>d</sup>, G. Casse<sup>b</sup>,  
I. Dawson<sup>a</sup>, D. Ferrère<sup>e</sup>, C.M.D. Grigson<sup>a</sup>, D. Morgan<sup>d</sup>, D. Robinson<sup>d</sup>

<sup>a</sup>Department of Physics and Astronomy, University of Sheffield, Sheffield S3 7RH, UK

<sup>b</sup>Oliver Lodge Laboratory, University of Liverpool, UK

<sup>c</sup>Max Planck Institut für Physik, Munich, Germany

<sup>d</sup>Cavendish Laboratory, University of Cambridge, UK

<sup>e</sup>DPNC, Université de Genève, Switzerland

Received 21 November 2000; received in revised form 12 February 2001; accepted 2 April 2001

## Abstract

Prototype ATLAS silicon microstrip detectors have been irradiated to the dose predicted for 10 years of LHC operation with 24 GeV protons at the CERN PS whilst cooled to the ATLAS design operating temperature. The detector currents were monitored during irradiation, which allows the predictions of bulk radiation damage parameterizations to be tested. Values for the damage constant  $\alpha$  and the rate of acceptor creation  $\beta$  have been calculated and are in agreement with those previously published for the irradiation of silicon diodes. © 2002 Elsevier Science B.V. All rights reserved.

PACS: 29.40.Wk; 61.82.Fk

Keywords: ATLAS; Radiation damage; Silicon microstrip detector

## 1. Introduction

The silicon microstrip detectors in the ATLAS Semiconductor Tracker (SCT) [1] will be subject to unprecedented levels of radiation; simulations have predicted that the inner layers of the SCT will receive approximately  $1.4 \times 10^{14}$  1 MeV equivalent neutrons per  $\text{cm}^2$  in the 10 year lifetime of the experiment [2]. The majority of this

radiation is due to charged hadrons from the primary interaction [3], therefore detectors should be irradiated with charged hadrons to address both ionisation and displacement damage. The 24 GeV primary proton beam from the CERN Proton Synchrotron (CPS) has been chosen to perform a series of detector irradiations as it is of sufficient intensity to enable the target fluence to be reached within a reasonable time scale.

During irradiation detector currents are recorded automatically and this has provided an opportunity to study the evolution of detector currents during proton irradiation, at

\*Corresponding author. Tel.: +44-114-222-3567; fax: +44-114-272-8079.

E-mail addresses: r.s.harper@sheffield.ac.uk (R.S. Harper).

temperatures similar to those foreseen for the ATLAS SCT. Comparisons can then be made with the predictions of bulk radiation damage parameterizations derived from post irradiation studies of silicon diodes and the values for the constants of these parameterizations determined specifically for ATLAS microstrip detectors.

## 2. ATLAS silicon detectors and the irradiation facility

The ATLAS SCT will consist of approximately 16 000 individual detectors, arranged in modules of four detectors into four cylindrical barrel layers in the central regions and 18 discs for the forward regions [1]. The detectors in the barrel are rectangular in shape having dimensions of 64 mm × 63.5 mm with an active area of 62 mm × 61.5 mm. The forward discs consist of five different designs of wedge shaped detectors, each of a similar area to the barrel detectors. A p-in-n design has been chosen, each detector having 770 AC coupled strips with an 80 μm pitch.

To enable a large number of detectors to be irradiated efficiently a dedicated irradiation facility has been established in the East Experimental Hall of the CPS [4,5]. A primary beam is used to irradiate the detectors with 24 GeV protons, which are incident on the detectors in approximately 400 ms spills, each containing between 20 and  $40 \times 10^{10}$  protons. With 1–3 spills being received per 14 s CPS super-cycle and a beam spot size of approximately 2 cm by 2 cm the beam intensity is  $2 - 9 \times 10^9$  p cm<sup>-2</sup> s<sup>-1</sup>. Because the detectors have a larger area than the beam it is necessary to scan them through it to achieve a uniform irradiation, thus reducing the effective intensity of the beam and increasing irradiation times. The target fluence for proton irradiation is  $3 \times 10^{14}$  p cm<sup>-2</sup>, derived from the predicted 1 MeV equivalent neutron fluence using a proton hardness factor of 0.68 and a 50% over estimation (recent results [6] suggest a proton hardness factor of 0.62, implying a target fluence for proton irradiation of  $3.4 \times 10^{14}$  p cm<sup>-2</sup>. However the target fluence of  $3 \times 10^{14}$  p cm<sup>-2</sup> has been retained for consistency across irradiations). This

fluence can be achieved in between 6 and 14 days depending upon beam conditions. The received fluence is measured using a secondary emission monitor upstream of the irradiation facility calibrated by the activation of aluminium foils [7].

During irradiation, the detectors are kept in a constant environment held at or below the ATLAS SCT design operating temperature of  $-7^\circ\text{C}$ . This is achieved by containing the detectors in a thermally insulated Styrofoam enclosure cooled by the passage of an antifreeze-water coolant mixture through heat exchangers. A uniform temperature and a dry atmosphere are maintained through the use of flat pack blower fans and a constant flow of dry nitrogen. Temperatures within the enclosure are monitored at several positions using pt100 thermistors. The thermal enclosure is situated on an x–y stage which is used to scan the detectors through the beamline, with a motion program that ensures the detectors receive a uniform fluence across their whole area. Each detector is biased independently with the strip metal and underlying implanted strips connected to ground and the backplane held at 100 V. The guard rings are floating. Detector currents are monitored and recorded automatically with a current measurement for each detector being taken every 1–3 min for the duration of the irradiation.

## 3. Radiation damage of silicon

Irradiation of silicon detectors by charged particles causes damage in both the bulk and the dielectric layer. Bulk damage has two effects on the detector: a change in the effective carrier density  $N_{\text{eff}}$  causing the full depletion voltage to change [8] and an increase in the leakage current due to the creation of deep traps which enhance the generation current [9]. The change in effective carrier density has been parameterized by

$$N_{\text{eff}}(\phi) = N_{\text{eff}}(0)e^{-c\phi} - \beta\phi. \quad (1)$$

The first term describes the removal of donors and the second term the creation of acceptors:  $N_{\text{eff}}(0)$  is the initial effective carrier density,  $c$  is the rate of donor removal and  $\beta$  is the rate of acceptor creation. The increase in leakage current has been

parameterized by

$$\Delta I = \alpha \phi \text{ Vol} \quad (2)$$

where  $\Delta I$  is the change in bulk detector leakage current,  $\alpha$  is the damage constant,  $\phi$  is the fluence and Vol is the active volume of the detector.

#### 4. Detector currents during irradiation

To predict the leakage current using bulk radiation damage parameterizations it is necessary to combine the effects of both the change in effective carrier density and the increase in leakage current. This is best done by considering the low fluence and high fluence regions separately. The pre-irradiation full depletion voltage for a 300  $\mu\text{m}$  thick detector is typically 60–80 V. The detectors are held at a constant bias of 100 V and are thus fully depleted when irradiation begins. The donor removal term in Eq. (1) initially causes the effective carrier density, and hence the full depletion voltage, to decrease and the detector remains fully depleted with a constant active volume. Therefore Eq. (2) implies that a linear relationship between detector current and fluence should be observed at low fluences (assuming the initial detector current to be negligible; initial currents of  $I_0 \approx 0.5 \mu\text{A}$  are observed).

At high fluences (above approximately  $10^{14} \text{ p cm}^{-2}$ ) the acceptor creation term in Eq. (1) dominates and to a good approximation  $|N_{\text{eff}}(\phi)| = \beta\phi$ . This results in a full depletion voltage greater than the applied bias voltage, the detector is no longer fully depleted and the active volume of the detector is now a function of fluence:

$$\text{Vol} = Aw = A \sqrt{\frac{2\varepsilon V_{\text{bias}}}{e |N_{\text{eff}}|}} = A \sqrt{\frac{2\varepsilon V_{\text{bias}}}{e \beta\phi}} \quad (3)$$

where  $A$  is the area of the detector,  $w$  is the depleted width of the detector,  $\varepsilon$  is the dielectric constant of silicon,  $e$  is the electron charge and  $V_{\text{bias}}$  is the bias voltage applied to the detector. Thus from Eq. (2) the detector current at high fluence should be given by

$$I = \alpha A \sqrt{\frac{2\varepsilon V_{\text{bias}}}{e \beta}} \phi^{0.5}. \quad (4)$$

Recent studies of irradiated diodes have shown the existence of a “double-junction”, with a small depleted n-type region on the  $\text{p}^+$  (strip) side as well as the expected depleted p-type region on the  $\text{n}^+$  (backplane) side [10,11]. However, the contribution of the extra depleted region to the overall depleted volume is expected to be small, therefore the above analysis neglects it and assumes that an under-depleted detector with depleted width  $w$  is equivalent to a fully-depleted detector of thickness  $w$ .

For the irradiation considered here 12 full-sized  $300 \pm 15 \mu\text{m}$  thick detectors from three different manufacturers (two detectors from manufacturer 1, five from manufacturer 2 and five from manufacturer 3) were irradiated to the target fluence of  $3 \times 10^{14} \text{ p cm}^{-2}$  whilst reverse-biased at 100 V. All of the detectors were manufactured on  $\langle 111 \rangle$  orientation substrate with resistivity of 2–5  $\text{k}\Omega \text{ cm}$ , and were a mixture of barrel and one of the wedge designs. The irradiation took 5.9 days and was performed at an ambient temperature of  $-10.0 \pm 0.1^\circ\text{C}$ . The measured detector currents have been normalised to  $-10.0^\circ\text{C}$  to take into account small temperature fluctuations in the thermal enclosure. Fig. 1 shows the current–fluence profile for a typical detector: the decrease in current observed at a fluence of approximately  $1.5 \times 10^{13} \text{ p cm}^{-2}$  was due to a period without beam. The origin of this decrease is unclear at present, although three options have been considered: leakage current annealing; discharge of the oxide layer or relaxation of the detector; photo-current caused by the decay of radioactive isotopes in the irradiation area.

The distinction between the low and high fluence regions is clearly shown and the exact relationships between current and fluence can be found with a fit to a graph of  $\log_{10}(I)$  against  $\log_{10}(\phi)$ . The low-fluence fit was performed for fluences between  $5 \times 10^{12}$  and  $2 \times 10^{13} \text{ p cm}^{-2}$ , and the high-fluence fit for fluences between  $1.5 \times 10^{14}$  and  $2.5 \times 10^{14} \text{ p cm}^{-2}$ . All of the detectors are compatible with the predicted  $I \propto \phi$  low-fluence behaviour: the mean of all 12 detectors is  $I_{\text{low}\phi} \propto \phi^{1.01 \pm 0.01}$ . However this is not the case for the expected high-fluence behaviour of  $I \propto \phi^{0.5}$ . Whilst the detectors from manufacturer 2 do agree

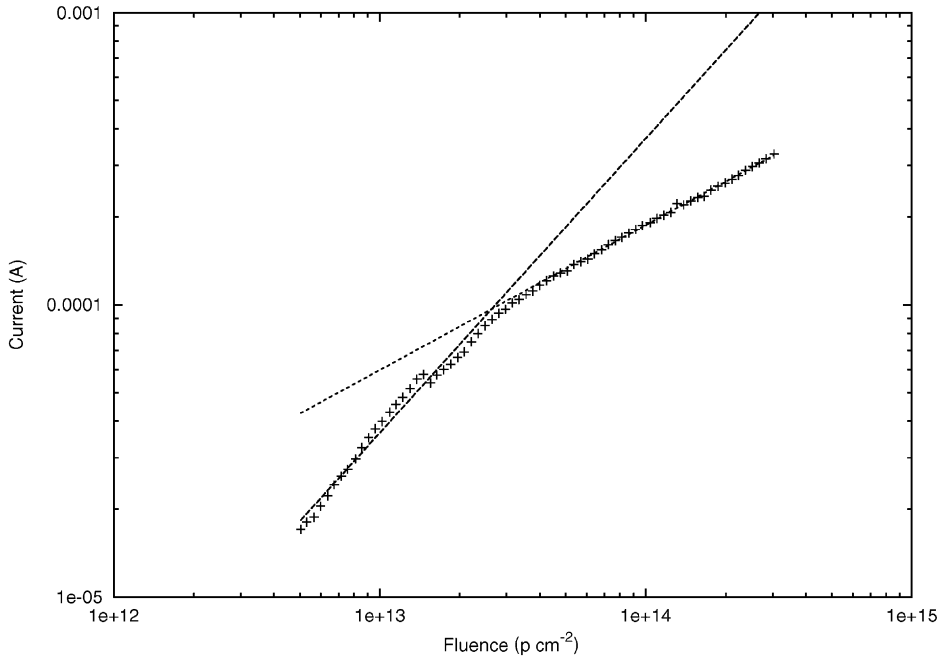


Fig. 1. Current profile for a detector biased at 100 V.

with this (the mean is  $I_{\text{high}\phi} \propto \phi^{0.502 \pm 0.002}$ ), the other detectors follow a relationship with a smaller power of the fluence: the mean for detectors from manufacturer 1 is  $I_{\text{high}\phi} \propto \phi^{0.417 \pm 0.006}$  and for detectors from manufacturer 3  $I_{\text{high}\phi} \propto \phi^{0.428 \pm 0.007}$ . This may indicate the presence of another effect in addition to the expected bulk radiation damage.

### 5. Determining the bulk radiation damage parameters

To model how the current changes as detectors are irradiated it is necessary to calculate the constants of the radiation damage parameterizations in Eqs. (1) and (2). At low fluences the damage constant  $\alpha$  can be derived by fitting  $I = X\phi$  to the current-fluence data and the rate of acceptor creation  $\beta$  can be calculated by fitting  $I = Y\phi^{0.5}$  to the data at high fluences. It is not possible to derive any information about the constant  $c$  in the donor removal term of Eq. (1) because this is only significant at low fluences, when the detectors

are fully depleted and only the linear increase in current governed by  $\alpha$  is seen. The average values of  $\alpha$  and  $\beta$  found at a temperature of  $-10.0^\circ\text{C}$  for detectors from the three different manufacturers are given in Table 1. The same data ranges were used to calculate these values as were used in the previous section. A systematic error has been included on  $\alpha$  to take into account the difficulty in fitting to the low-fluence data due to the period without beam and subsequent fall in current at  $1.5 \times 10^{13} \text{ p cm}^{-2}$ . This has been derived from the difference between values of  $\alpha$  found before and after this fluence.

The  $\alpha$  and  $\beta$  parameters calculated can be used in conjunction with Eqs. (1) and (2) to model the evolution of detector currents with fluence. The results can be seen for detectors from manufacturer 2 in Fig. 2 and for detectors from manufacturer 3 in Fig. 3. It is apparent that whilst Fig. 2 shows excellent agreement between the model and data for manufacturer 2 detectors, Fig. 3 shows that the model, although broadly representing the magnitude of the data, has a slightly different

Table 1

The average values of  $\alpha$  and  $\beta$  for detectors from each manufacturer

|                |  |   |
|----------------|--|---|
| Manufacturer 1 | $\alpha = (2.99 \pm 0.28) \times 10^{-18} \text{ A cm}^{-1}$ | $\beta = 0.052 \pm 0.007 \text{ cm}^{-1}$ |
| Manufacturer 2 | $\alpha = (3.24 \pm 0.18) \times 10^{-18} \text{ A cm}^{-1}$ | $\beta = 0.061 \pm 0.005 \text{ cm}^{-1}$ |
| Manufacturer 3 | $\alpha = (3.34 \pm 0.18) \times 10^{-18} \text{ A cm}^{-1}$ | $\beta = 0.060 \pm 0.005 \text{ cm}^{-1}$ |

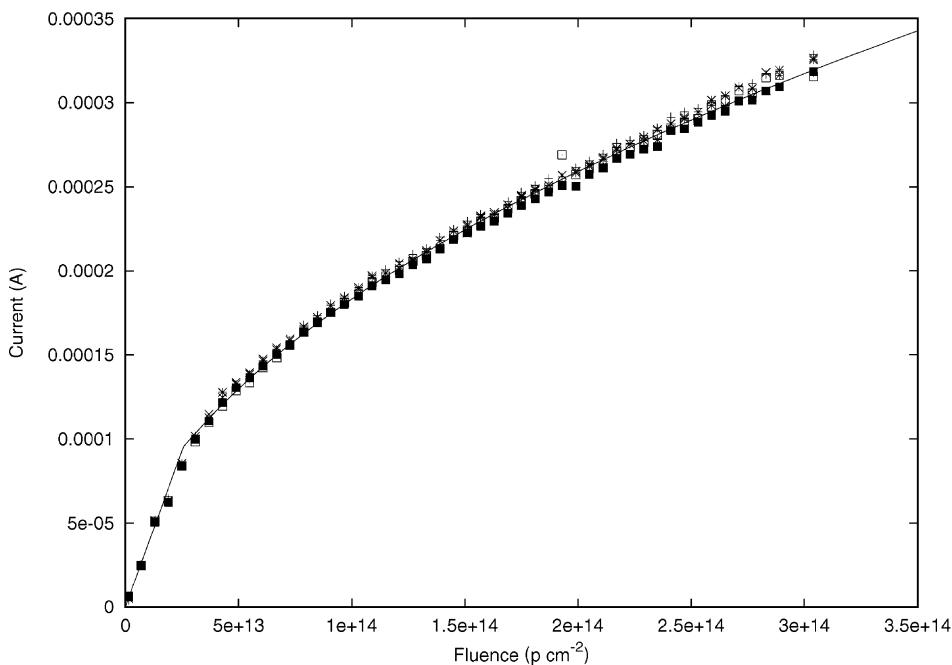


Fig. 2. Current data and predictions of model for detectors from manufacturer 2.

shape (this is also the case for the detectors from manufacturer 1). This is not entirely unexpected, as the calculation of the  $\beta$  parameter assumes a relationship between current and fluence of  $I \propto \phi^{0.5}$ , whereas in the previous section this relationship was found not to be true for detectors from manufacturers 1 and 3.

## 6. Discussion

In order to compare the values of the damage constant  $\alpha$  and the rate of acceptor creation

$\beta$  found here with previously published results the average values from all 12 detectors, have been used. The average value of the damage constant  $\alpha$  is

$$\alpha(-10^\circ\text{C}) = (3.24 \pm 0.12) \times 10^{-18} \text{ A cm}^{-1}.$$

It is standard to normalise values of  $\alpha$  to a temperature of  $20^\circ\text{C}$  for the purposes of comparison, using [9]

$$I(T) \propto T^2 \exp\left(\frac{-E_g}{2k_B T}\right) \quad (5)$$

where  $E$  is the effective energy gap (a value of

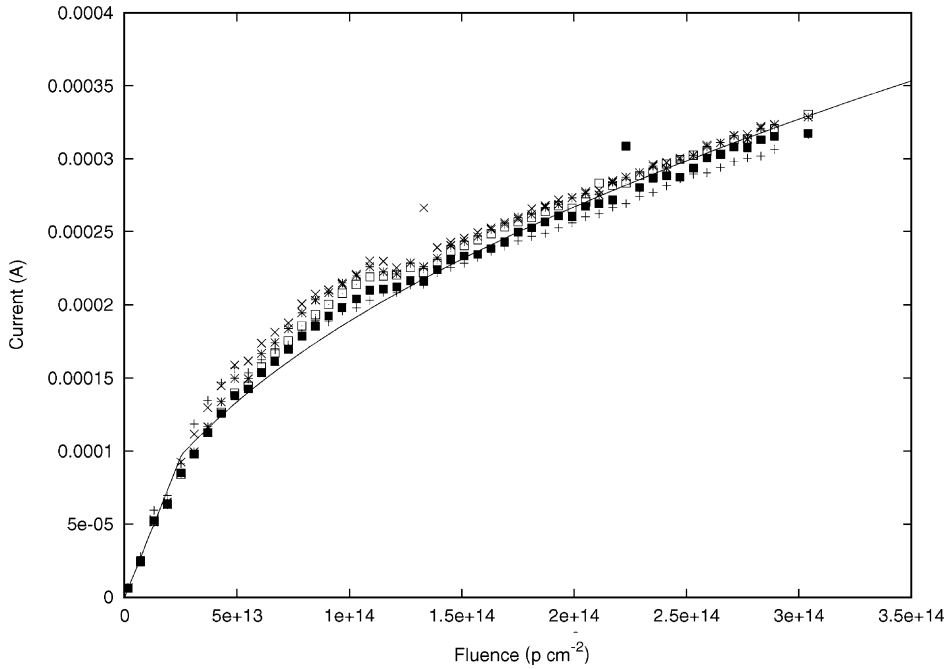


Fig. 3. Current data and predictions of models for detectors from manufacturer 3.

1.12 eV has been used) and  $k_B$  is Boltzmann's constant. The value of  $\alpha$  normalised to 20°C is

$$\alpha(20^\circ\text{C}) = (5.03 \pm 0.20) \times 10^{-17} \text{ A cm}^{-1}.$$

This compares favourably with the results of other groups for the irradiation of silicon diodes at the CPS, for example:  $\alpha(20^\circ\text{C}) = (5.0 \pm 0.4) \times 10^{-17} \text{ A cm}^{-1}$  [12] and  $\alpha(20^\circ\text{C}) = (5.4 \pm 0.5) \times 10^{-17} \text{ A cm}^{-1}$  [13]. Both of these values have been corrected for self annealing. It is expected that only a small amount of leakage current annealing will have taken place for the measurement presented here due to the low temperature and since the calculation of  $\alpha$  was performed only for data collected within the first 20 h of irradiation.

The average value for rate of acceptor creation  $\beta$  is  $\beta(-10^\circ\text{C}) = (0.059 \pm 0.003) \text{ cm}^{-1}$ .

Recent values for the  $\beta$  parameter have been obtained after annealing the irradiated samples for 4 min at 80°C, which takes the sample to a point where beneficial annealing is completed and

reverse annealing has yet to begin, i.e. only the stable component of the effective carrier density is measured. For example,  $\beta(4 \text{ min}/80^\circ\text{C}) = 0.0154 \text{ cm}^{-1}$  [14]. However, for the case of  $\beta(-10^\circ\text{C})$  as found here, the time constants for the beneficial annealing of the radiation induced change in the effective carrier density at  $-10^\circ\text{C}$  are much greater than the irradiation time (for example 439.9 days [15] and 306 days [16]). Therefore, only a small amount of beneficial annealing will have occurred and a larger value of  $\beta$  is expected. A previous analysis of diodes irradiated with protons whilst cooled to low temperatures [17] found  $\beta(0^\circ\text{C}) = 0.047 \pm 0.0002 \text{ cm}^{-1}$  and  $\beta(-20^\circ\text{C}) = 0.109 \pm 0.001 \text{ cm}^{-1}$ . These values would appear to be consistent with that found here for irradiation at  $-10^\circ\text{C}$ .

As previously noted, the analysis performed here relies upon the assumption that an under-depleted detector with depleted width  $w$  is equivalent to a fully-depleted detector of thickness  $w$ , neglecting any contribution from a double-junction effect.

Whilst the data from the manufacturer 2 detectors would certainly seem to support this assumption, the fact that the manufacturer 3 detectors do stray from the expected  $I \propto \phi^{0.5}$  high-fluence behaviour may indicate some contribution from an additional depleted region. Further work needs to be undertaken to clarify this point.

## 7. Conclusions

Prototype full-sized ATLAS silicon microstrip detectors have been irradiated to the predicted 10 year dose using a beam of 24 GeV protons extracted from the CERN PS. The detectors were cooled and held under bias during irradiation and detector currents were recorded throughout. The detector currents have been compared with those predicted by a model derived from bulk radiation damage parameterizations. Values of the damage constant  $\alpha$  and the rate of acceptor creation  $\beta$  for irradiation with 24 GeV protons at  $-10^\circ\text{C}$  have been calculated. The value of  $\alpha$  normalised to a temperature of  $20^\circ\text{C}$  was found to be in good agreement with those previously published for proton irradiation. The value of  $\beta$  was found to be higher than values quoted after annealing for 4 min at  $80^\circ\text{C}$ , which is expected as the time constants for beneficial annealing at a temperature of  $-10^\circ\text{C}$  are much greater than the irradiation time, hence only a small amount of beneficial annealing will have occurred.  $\beta(-10^\circ\text{C})$  found here is compatible with values previously found for diodes irradiated at low temperatures.

## Acknowledgements

The authors would like to acknowledge E. Tsemelis, T. Ruf and all of the CPS staff for

their contribution to the smooth running of the irradiation facility. They would also like to thank F. Lemeilleur and M. Glaser from RD48, R. Nicholson of the University of Sheffield, A. Fürtjes of CMS and R. Fortin of CERN. This work has been partially supported by the Particle Physics and Astronomy Research Council, UK.

## References

- [1] Y. Unno, Nucl. Instr. and Meth. A 453 (2000) 109.
- [2] ATLAS Inner Detector Technical Design Report, CERN/LHCC/97-17, 1997.
- [3] I. Dawson, Nucl. Instr. and Meth. A 453 (2000) 461.
- [4] D. Morgan, Semiconductor detectors for the inner tracker of the ATLAS experiment at CERN, Ph.D. Thesis, University of Sheffield, Sheffield, UK, 2000.
- [5] M. Glaser, et al., Nucl. Instr. and Meth. A 426 (1999) 72.
- [6] G. Lindström, et al., Nucl. Instr. and Meth. A 465 (2001) 60.
- [7] K. Bernier, et al., Calibration of secondary emission monitors of absolute proton beam intensity in the CERN SPS North area, CERN 97-07, 1997.
- [8] J.A.J. Matthews, et al., Nucl. Instr. and Meth. A 381 (1996) 338.
- [9] G. Lindstrom, et al., Nucl. Instr. and Meth. A 426 (1999) 1.
- [10] G. Casse, et al., Nucl. Instr. and Meth. A 426 (1999) 140.
- [11] D. Menichelli, et al., Nucl. Instr. and Meth. A 426 (1999) 135.
- [12] S.J. Bates, The effects of proton and neutron irradiations on silicon detectors for the LHC, Ph.D. Thesis, University of Cambridge, Cambridge, UK, 1993.
- [13] S.J. Bates, et al., IEEE Trans. Nucl. Sci. 43 (3) (1995) 1002.
- [14] A. Ruzin, Nucl. Instr. and Meth. A 447 (2000) 116.
- [15] H.-J. Ziöck, et al., Nucl. Instr. and Meth. A 342 (1994) 96.
- [16] M. Moll, Radiation damage in silicon particle detectors—microscopic defects and macroscopic properties, Ph.D. Thesis, University of Hamburg, Hamburg, Germany, 1999.
- [17] F. Lemeilleur, et al., Nucl. Instr. and Meth. A 360 (1995) 438.